

Effects of Photo Illumination on Diamond Based DDR IMPATT Diode Operating at MM-wave Frequency Band

B. Chakrabarti, D. Ghosh, M. Mitra

Abstract: *The effect of photo illumination on the d.c and small signal performance of diamond based IMPATT diode operating at W-band is investigated using a modified double iterative simulation method. Under optical illumination additional photo generated carriers are produced in the device which modulates the admittance and negative resistance properties of the diode. It is found that the operating frequency shift upward accompanied by degradation of negative conductance, negative resistance, quality factor and output power density level under photo illumination. Decrement in the values of negative conductivity by 19.2 % and in total negative resistance by 21 % has been observed when the diode is exposed to photo illumination. It is also established that the d.c properties of the diode become inferior as the intensity of optical illumination increases.*

Key words: *Diamond IMPATT, Photo illumination, W-band, Negative Conductivity, Resistivity.*

I. INTRODUCTION

Impact Avalanche transit time diodes (IMPATT) are the most powerful solid state sources at mm and sub mm (THz) wave frequencies and are largely used in various civilian and space communication systems as well as in high power radars, missile seekers, and so forth. Conventional Si- and GaAs- based mm-wave IMPATTs are found to be reliable, but these are limited by power and operating frequencies, due to limitations of their inherent material parameters. Extensive research in being carried out to meet the gradual demand for high power solid-state sources which can operate at high temperature. One approach is to employ power combining technique to increase the output power of the IMPATT devices, but practical realization of such combination is a very difficult issue.

The other option is to develop IMPATT devices from wide-band gap semiconductor materials which are having material properties conducive for high power, high frequency, and high temperature operations. Silicon carbide (SiC) and Gallium Nitride (GaN) are two such semiconductors. The use of these wide band gap semiconductors for microwave and millimeter wave power applications have been discussed by many researchers [1-7]. The interest in Diamond has high power microwave and millimeter wave source has grown with the improvements in epitaxial growth, rectifying and ohmic contacts. Fujimori et al.

[8], Okano et al. [9] have created new interest among the researchers in developing Diamond devices that will work at high temperature and high frequency. With the advent of diamond CVD process [10] and etching process [11] realization of diode with diamond as the base material have become possible. Diamond has been recognized as having many superior material properties for possible future electronic devices, such as high breakdown field, high saturation velocity, high carrier mobilities and highest thermal conductivity of all materials. The mobilities of Diamond are very high with only the electron mobility of GaAs exceeding those values. High carrier mobilities are desirable for fast response and high frequency electronic devices. High value of thermal conductivity is an essential requirement for power electronics devices which suffer from a high generation of heat. Traditional power electronic devices have to be kept on heat sinks to prevent the device from thermal damage. For Diamond based devices that may not necessary as it has the highest reported thermal conductivity. Diamond also has many additional advantages over other wide band gap semiconductor materials such as Gallium nitride (GaN) and Silicon carbide (SiC). The growth of the epitaxial layer of Diamond in a CVD process is in many ways simpler than it is to grow for other wide band gap semiconductor materials. This is due to the simpler structure of Diamond, consisting of carbon atoms only. Again polyatomic materials such as SiC and GaN exist in many hundred different crystalline structures. Epitaxy of SiC is riddled with a particular problem, the formation of tubular channels, called micro pipes [12] during growth which does not exist for Diamond. In addition to these growing of diamond in a CVD process is advantageous as the raw materials are cheap compared to SiC and GaN. The first ever millimeter wave performance of diamond IMPATT was simulated and compared with that of conventional Si, GaAs, and InP IMPATTs at different mm wave frequency bands by Trew et al. [13], which established the superiority of diamond based IMPATT in terms of efficiency and output power. Later Tao Wu [14] has also analyzed the performance of diamond IMPATT in the terahertz frequency band taken into consideration different diode structures.

Controlling of the dynamic properties of IMPATT diode by external agencies such as photo radiation can have tremendous application in space communication systems. The performance of an IMPATT oscillator used as a source in spacecrafts may change appreciably when it is subjected to interstellar radiation. In the basic process a photon (due to optical or other radiation) of energy $h\nu$ greater than the band gap (E_g) energy of the semiconductor is absorbed at the edges of depletion layer additional electron-hole pairs

Manuscript received on May, 2013.

B. Chakrabarti, Department of ECE, Bengal Institute of Technology, Kolkata-150, India .

D. Ghosh, Dept. of ECE, Future Institute of Engineering & Management, Kolkata-150, India.

M. Mitra, Dept. of E&TC Engg., Bengal Engineering & Science University, Shibpur, Howrah 711103, W.B., India.

are created. The photo generated minority carriers add up with temperature generated minority carriers and there by enhance the total leakage current that alters the avalanche phase delay of the diode and modify the d.c and small signal properties of the diode. However, detailed small signal and d.c analysis results of diamond based IMPATT diode are not available in the current literature which is very much necessary considering the future prospect of diamond as mm-wave power source. The authors have performed theoretical investigations on the role of external radiation in modulating the admittance and negative resistivity properties of Diamond IMPATT diode operating at W-band (75 GHz-110 GHz) and compared the performances under different intensity of optical illumination. Some experimental [15] and theoretical [3, 4] studies on the optically illuminated IMPATT diode revealed the degradation in performance in terms of output power and efficiency of the diode.

II. SIMULATION METHODOLOGY AND MATERIAL PARAMETERS

For the present analysis, a flat-profile DDR (n⁺⁺n p p⁺⁺) structure is considered, where n⁺⁺ and p⁺⁺ are highly doped substrates, and n, p are the epilayers. In the dc method, the numerical computation starts at the field maxima near the metallurgical junction. The method is used by simultaneous solving Poisson’s and carrier current continuity equations at each point in the depletion layer. The dc electric field and normalized carrier currents density profile in the depletion layer are obtained by a double-iterative simulation technique described elsewhere [3]. The field boundary conditions are given as,

$$E(-W_n)=0 \quad \text{and} \quad E(W_p)=0 \tag{1}$$

Here -W_n and W_p represent the edges of the depletion layer in n and p regions, respectively.

The boundary conditions for normalized current density P(x), are given as,

$$P(-W_n) = (2/M_p - 1) \text{ and} \\ P(W_p) = (1 - 2/M_n) \tag{2}$$

Where M_n = J/J_{ns}, M_p = J/J_{ps}; J_{ns} and J_{ps} are electron and hole leakage current densities, M_n and M_p are hole and electron current multiplication factors, respectively. Again P = (J_p-J_n)/J, where J_p = hole current density, J_n = electron current density, and J total current density. The breakdown voltage of the diode is obtained by integrating the electric field profile over the entire depletion layer width; that is

$$V_B = \int_{-W_n}^{W_p} E(x)dx \tag{3}$$

The d.c to mm wave conversion efficiency is calculated from the approximate formula

$$\eta (\%) = (V_D) \cdot (100/\pi) / V_B \tag{4}$$

Where V_D is the voltage drop across the drift region. Also V_D = V_B - V_A, where V_A is the voltage drop across the avalanche region.

The range of frequencies over which the diode exhibits negative conductance can easily be computed by Gummel-Blue method [16]. The resistive part R(x, ω) and reactive part X(x, ω) are obtained by splitting the diode impedance Z(x, ω) using Gummel-Blue method and thus two different equations are framed [3]. Then, by using modified Runga-Kutta method [17] the solutions of these two equations are found following a double iterative simulation scheme. The small signal parameters like negative conductance(-G), susceptance (B), impedance (Z) of the diode and the range of frequencies over which the diode exhibits negative

conductance are found after satisfying the boundary conditions derived elsewhere [18,19].The diode total negative resistance (-Z_R) and reactance (-Z_x) at a particular frequency can be determined from numerical integration of the resistivity (-R(x)) and reactivity (-X(x)) profiles over the entire depletion layer.

Thus,

$$-Z_R = \int_{-W_n}^{W_p} -R \, dx \text{ and } -Z_X = \int_{-W_n}^{W_p} -X \, dx \tag{5}$$

The diode total impedance Z is obtained by,

$$Z_{total} = \int_{-W_n}^{W_p} Z(x, \omega)dx = -Z_R + jZ_X \tag{6}$$

The diode admittance is expressed as

Y = 1/Z = -G + jB = 1/(-Z_R + jZ_x) and diode total negative conductance and susceptance have been calculated from the following formulas

$$\text{or, } G = -Z_R / ((Z_R)^2 + (Z_x)^2) \quad \text{and} \\ B = Z_x / ((Z_R)^2 + (Z_x)^2) \tag{7}$$

G and B are both normalized to the diode area.

The small signal quality factor (Q_p) is defined as the ratio of the imaginary part of the admittance (B) to the conductance (G) (at the peak frequency), i.e.

$$-Q_p = (B_p / -G_p) \tag{8}$$

At f_p, the maximum RF power (P_{RF}) from the device is obtained from the expression.

$$P_{RF} = (V_{RF}^2) \cdot (-G_p) \cdot A / 2 \tag{9}$$

The area (A) of the diode is considered to be 5x10⁻¹¹ m². Under small signal condition V_{RF} (the amplitude of the RF swing) is taken as V_B/5.

When the IMPATT diode is exposed to interstellar radiation, the performance of IMPATT oscillator changes appreciably due to the absorption of optical photon of energy greater than the band gap energy of the semiconductor. The photo generated minority carriers add up with temperature generated minority carriers and there by enhance the total leakage current that alters the avalanche phase delay of the diode and modify the performance of the diode.

Normally the leakage current (J_s) under reverse bias condition is due to the thermally generated electrons and holes. Therefore

$$J_s = J_{ns}(th) + J_{ps}(th) \tag{10}$$

So the current multiplication factors at the two edges of the depletion layers are given as

$$M_{n/p} = J / [J_{ns}(th) \text{ or } J_{ps}(th)] \tag{11}$$

Where J = bias current density. Therefore M_{n/p} can be considered almost infinity. Thus, the enhanced leakage current under optical illumination lowers the magnitude of M_{n/p}.

Under optical illumination, the electron current multiplication factor reduces to

$$M_n = J_o / [J_{ns}(th) + J_{ns}(opt)] \tag{12}$$

Where J_{ns}(opt)= leakage current due to photo generated electrons.

In order to assess the role of leakage current in controlling the dynamic properties of Diamond IMPATT oscillators, simulation studies are carried out by the authors considering three different values of M_n (keeping M_p very high ~10⁶)

In the simulation method, the authors have considered latest reported values of material parameters and their realistic variation with electric field and temperature.

The Monte Carlo simulated values of drift velocity and mobility of charge carriers [20, 21] in Diamond are considered for the simulation experiment. Because of the lack of experimental values of ionization rates (α_n , α_p) in Diamond the authors have considered the theoretical predicted values [13] in the present study.

Table 1: Structural parameters of flat profile DDR Diamond IMPATT diode

| $W_n(\mu\text{m})$ | $W_p(\mu\text{m})$ | $N_D(10^{23}\text{m}^{-3})$ | $N_A(10^{23}\text{m}^{-3})$ | $J_0(10^8\text{Am}^{-2})$ |
|--------------------|--------------------|-----------------------------|-----------------------------|---------------------------|
| 0.930 | 0.812 | 0.31 | 0.33 | 1 |

III. RESULT AND DISCUSSIONS

The operating current density (J_0), doping levels and the corresponding non punch through depletion layer widths (W_n and W_p) of n- and p-region for W-band (75-110 GHz) operation are given in Table 1. The dc parameters of the Diamond IMPATTs obtained from computer analysis under different depth of optical illuminations are presented in Table 2.

Table 2: D.C properties of Diamond-IMPATT diode under photo-illumination

| M_p | M_n | $E_m(10^8\text{Vm}^{-1})$ | $x_0(10^{-10}\text{m})$ | $V_B(\text{V})$ | $V_A(\text{V})$ | $\eta(\%)$ |
|--------|---------------|---------------------------|-------------------------|-----------------|-----------------|------------|
| 10^6 | $M_{n1}=10^6$ | 0.936 | 0.875 | 92.6 | 38.8 | 18.48 |

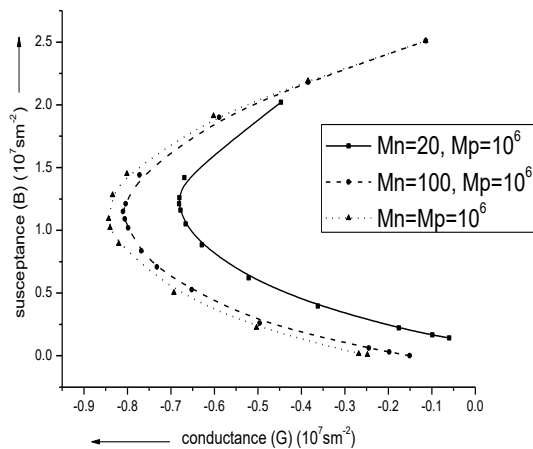


Figure 1: Admittance plot for diamond DDR IMPATT diode under optical illumination

The effects of electron dominated photo currents on the small signal behavior of Diamond based IMPATT are presented in table 3. The results clearly show that as the value of M_n becomes small the magnitude of the peak negative conductance $|-G_p|$ decreases. At the same time the peak operating frequency (f_p) shifts towards higher frequencies with the lowering of M_n . The output data of the illuminated diode indicates that the magnitude of peak negative conductance ($-G_p$) decreases by 19.2 % when M_n reduces from 10^6 to 20. The same trend can also be observed in figure 1 which shows the variation of conductance ($-G$) and susceptance (B) with frequency. Figure 2 shows the profiles of negative resistivity at the peak frequencies (f_p) corresponding to different values of M_n . The negative resistivity profile $R(x)$ at the optimum frequency provides

| | | | | | |
|---------------|-------|-------|------|------|-------|
| $M_{n2}=10^2$ | 0.935 | 0.813 | 91.6 | 38.7 | 18.37 |
| $M_{n3}=20$ | 0.931 | 0.563 | 90.6 | 38.5 | 18.29 |

The magnitude of the peak electric field (E_m) is found to be highest under no illumination condition ($M_n=10^6$) and it decreases as the depth of illumination increases that is M_n decreases. It is also evident from table 2 that the avalanche zone is much more localized for Diamond based IMPATT when the diode is not exposed to optical illumination. The narrower avalanche zone leads to higher ratio of drift voltage (V_D) to breakdown voltage (V_B) which in turn characterizes higher conversion efficiency (η). The diode therefore exhibits highest conversion efficiency of 18.48% when $M_n=10^6$ and lowest conversion efficiency of 18.29% when $M_n=20$. The breakdown voltage (V_B) decreases slightly with the lowering of M_n from 10^6 to 20. Therefore considering the d.c performance in term of breakdown voltage, efficiency it is observed that Diamond based IMPATTs give degraded performance under optical illumination.

Table 3: Variations of small signal parameters of Diamond DDR IMPATT diode under photo-illumination

| M_p | M_n | $f_p(\text{GHz})$ | $-G_p(10^7\text{Sm}^{-2})$ | Q_p | $-Z_R(10^7\Omega\text{m}^{-2})$ | $-Z_x(10^7\Omega\text{m}^{-2})$ | $P_{\text{RF}}(\text{W})$ |
|--------|---------------|-------------------|----------------------------|-------|---------------------------------|---------------------------------|---------------------------|
| 10^6 | $M_{n1}=10^6$ | 104 | 0.843 | 1.29 | 0.443 | 0.573 | 0.07 |
| | $M_{n2}=10^2$ | 105 | 0.801 | 1.43 | 0.407 | 0.580 | 0.067 |
| | $M_{n3}=20$ | 106 | 0.681 | 1.77 | 0.350 | 0.621 | 0.056 |

better insight into the region of depletion layer that contribute RF power. The computed $R(x)$ profile in each case is characterized by two negative resistivity peaks (R_{max}) almost in the middle of the drift layers. It can further be verified that the magnitude of the negative resistivity peak in the hole drift region (p-region) and electron drift region (n-region) are almost same for the diode. This may be due to similar value of charge carrier ionization (α_n & α_p) rates in diamond. Figure 3 also exhibits that due to lowering of M_n the negative resistivity peak values are reduced accompanied by a gradual shift in their positions from the middle of the drift region towards the n^{++} and p^{++} edges. Figure 3 shows the small signal impedance plot for the diode at the optimum frequency. The graph shows that the magnitude of $-Z_R$ is small compared to magnitude of $-Z_x$ at all frequencies. It is also evident from the figure 3 that the values of $|-Z_R|$ decreases as the values of M_n decreases whereas $|-Z_x|$ follows the reverse trend. Under optical illumination the total negative resistivity ($-Z_R$) value decreases by 21 % for Diamond diode as M_n changes from 10^6 to 20.

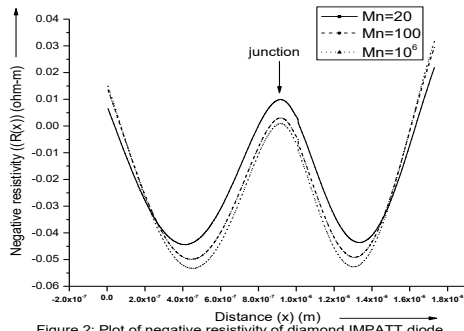


Figure 2: Plot of negative resistivity of diamond IMPATT diode

Taken into consideration the negative quality factor ($-Q_p$) it is further observed that Diamond based diode gives better response at W-band under no photo illumination condition ($M_n=10^6$).

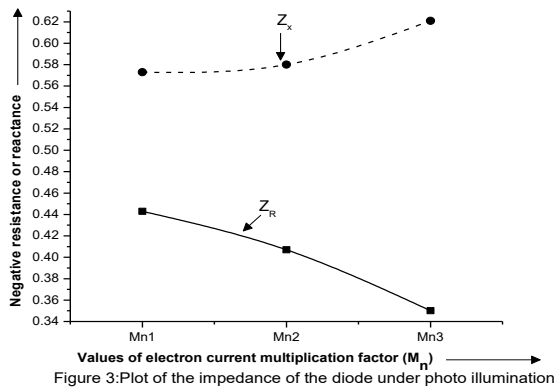


Figure 3: Plot of the impedance of the diode under photo illumination

The quality factor (Q_p) of Diamond IMPATT increases by 37 % as M_n reduces from 10^6 to 20. The present study also suggests that the RF power (P_{RF}) generated by Diamond IMPATT diode at W-band decreases as M_n decreases. The decreasing nature of P_{RF} with photo illumination can also be seen in figure 4. Therefore considering all these findings it can be predicted that the small signal performance of the Diamond IMPATT diode would be degraded severely when the diode is exposed to interstellar radiation.

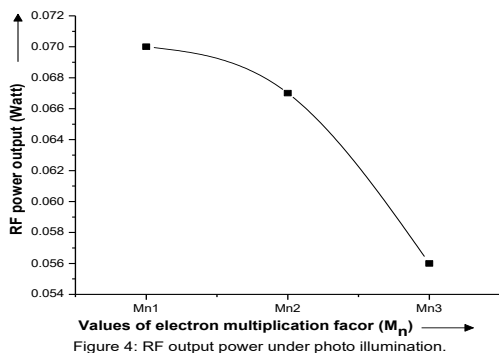


Figure 4: RF output power under photo illumination.

IV. CONCLUSION

The enhancement of leakage current by electron dominated photo current thus lead to a decrease of total negative resistance ($-Z_R$), peak negative conductance ($-G_p$), and output RF power (P_{RF}) along with a simultaneous upward shift of optimum operating frequency (f_p) and negative quality factor ($-Q_p$). In addition to this photo generated leakage current also modulates various d.c

properties such as efficiency (η), breakdown voltage (V_B) of the diode. The simulation results thus provide useful information regarding the optical control of the various d.c and small signal properties of Diamond based DDR IMPATT diode.

REFERENCES

- [1] V.V.Buniatyan and V.M.Aroutiounian, "Wide gap semiconductor Microwave devices", J.phys.D: Appl.phys. vol.40, no.20, pp.6355-6385.
- [2] I.Mehdi, G.I.Haddad, and R.K Mains, "Microwave and millimeter wave power generation in Silicon carbide Avalanche devices", J. Appl. Phys., 64(3), August 1988.
- [3] M.Mukherjee, N. mazumder, S.K.Roy, and K.Goswami, "GaN IMPATT diode: a photo-sensitive high power terahertz source", Semicond. Sci. Technol. (UK), vol.22, pp.1258-67,(2007).
- [4] M.Mukherjee, N. mazumder, and S.K.Roy, "Photosensitivity analysis of Gallium nitride and Silicon carbide terahertz IMPATT oscillators: comparison of theoretical reliability and study on experimental feasibility", Semicond. Sci. Technol. (UK), vol.22, pp.1258-67, (2007).
- [5] S.R.Pattanaik, G.N.Dash, and J.K.Mishra, "Prospects of 6H-SiC for operation as an IMPATT diode at 140GHz", Semicond. Sci. Technol., vol.20, pp.299-304, (2005).
- [6] B.Chakrabarti, D.Ghosh, M.Mitra " High Frequency Performance of GaN Based IMPATT Diodes", I.J.E.S.T., vol.3 No.8, August 2011.
- [7] D. Ghosh, B. Chakrabarti, M. Mitra "A Detailed Computer Analysis Of SiC And GaN Based IMPATT Diodes Operating at Ka, V And W Band", I.J.S.E.R., vol. 3 issue 2, 2012
- [8] N.Fujimori, T.Imai, and A.Do, "characterization of conducting Diamond films", Vacuum, vol.36, Issues 1-3, pp.99-102, 1986.
- [9] K.Okano, H. Naruki, Y.Akiba, T.Kurosu, M. Lida, and y. Hirose, "Synthesis of Diamond thin films having semiconductive properties", Jpa.J.Appl.phys. 27, L173-5, 1988.
- [10] P.W. May, "Diamond thin films: a 21st-century material", Phil. Trans. R. Soc. Lond. , vol. 358, no.1766, pp. 473-495, (2000).
- [11] D.S. Hwang, T. Saito, and N. Fujimori, "New etching process for device fabrication using diamond", Diamond and Related Materials, vol.13, pp.2207-2210, 2004.
- [12] V. Dmitriev, S.Rendakova, N.Kuznetsov, N.Savkina, A.Andreev, M.Rastegeava, M.Mynbaeva, and A. Morozov, "Large area silicon carbide devices fabricated on SiC wafers with reduced micropipe density", Materials science and Engineering, B 61-62, 446-449 (1999).
- [13] R.J.Trew, J.B.Yan, P.M.Mock, "The potential of Diamond and SiC electronic devices for microwave and millimeter wave power applications", Proc. IEEE, vol.79, No.5, May 1991.
- [14] T.Wu, "Diamond Schottky Contact Transit-time Diode for Terahertz Power Generation", Int. J. Infrared Milli. Waves, vol. 29, pp.634-640, 2008.
- [15] H.P.Vyas, R.J.Gutmann, and J.M.Borrego, "Effect of hole versus electron photocurrent on microwave-optical interactions in impatt oscillator", IEEE trans. Elect. Devices, vol.26, no.3, pp.232-234, 1979.
- [16] H.K.Gummel and J.L.Blue "Small Signal Theory of Avalanche Noise in IMPATT diodes", 1967 IEEE Trans.Electron Devices, vol.14, 569.
- [17] S.K.Roy, J.P.Banerjee, and S.P.Pati, " Numerical Analysis of semiconductor devices", (NASACODE IV) Dublin: Boole, 1985, P. 494.
- [18] M. Mukherjee, S.K. Roy, "Wide band gap III-IV nitride based avalanche transit time diode in terahertz regime: studies on the effects on punch through on high frequency characteristics and series resistance of the device ", Current Appl. Phys., vol.10, pp.646-651.
- [19] H.Eisele and G.I.Haddad, "Active microwave Devices in Microwave Semiconductor Device Physics ed S M Sze (New York)", p.343, 1997.
- [20] T.Watanabe, T.Teraji, T.Ito, Y.Kamakura, and K.Taniguchi, "Monte Carlo simulations of electron transport properties of diamond in high electric fields using full band structure", J. Appl. Phys., vol.95, No.9, May 2004.
- [21] Electronic Archive: New Semiconductor Materials, Characteristics and properties [online]. Available:

